

# Organolanthanide-Catalyzed Imine Hydrogenation. Scope, Selectivity, Mechanistic Observations, and Unusual Byproducts

Yasushi Obora, Tetsuo Ohta, Charlotte L. Stern, and Tobin J. Marks\*

Contribution from the Department of Chemistry, Northwestern University, Evanston, Illinois 60208-3113

Received October 30, 1996<sup>⊗</sup>

**Abstract:** In this paper we report the Cp'<sub>2</sub>Ln/Me<sub>2</sub>SiCp''<sub>2</sub>Ln-catalyzed (Cp' = η<sup>5</sup>-Me<sub>5</sub>C<sub>5</sub>; Cp'' = η<sup>5</sup>-Me<sub>4</sub>C<sub>5</sub>) hydrogenation of acyclic imines to yield the corresponding amines. At 190 psi of H<sub>2</sub>, the observed turnover frequencies (h<sup>-1</sup>) (100:1 substrate:catalyst ratio, Cp'<sub>2</sub>Ln, temperature (°C)) are (1) (*N*-benzylidene(methyl)amine, Ln = La, 50) 0.03; (Ln = Sm, 90) 1.0; (Ln = Sm + PhSiH<sub>3</sub>, 90) 2.2; (Ln = Lu, 90) 0.60; (2) (*N*-benzylideneaniline, Ln = Sm, 90) 0.10; (3) (*N*-benzylidene(trimethylsilyl)amine, Ln = Sm, 90) 0.40; (4) (*N*-(α-methylbenzylidene)(methyl)amine, Ln = Sm, 90) 0.20; (5) (*N*-(α-methylbenzylidene)(benzyl)amine, Ln = Sm, 90) 0.70. The stoichiometric reaction of *N*-benzylidene(methyl)amine with Cp'<sub>2</sub>SmCH(SiMe<sub>3</sub>)<sub>2</sub> or (Cp'<sub>2</sub>SmH)<sub>2</sub> yields an orthometalated Cp'<sub>2</sub>Sm-substrate complex which undergoes either hydrogenolysis/hydrogenation or competing C=N insertion of a second substrate molecule to yield a Cp'<sub>2</sub>Sm-imine-amido complex with a seven-membered chelate ring. The stoichiometric reaction of 2-methyl-1-pyrroline with Cp'<sub>2</sub>SmCH(SiMe<sub>3</sub>)<sub>2</sub> or (Cp'<sub>2</sub>SmH)<sub>2</sub> yields a Cp'<sub>2</sub>Sm-imine-amido complex in which two substrate molecules have been coupled to form a six-membered chelate ring (characterized by X-ray diffraction). The stoichiometric reaction of *N*-benzylidene(trimethylsilyl)amine with (Cp'<sub>2</sub>SmH)<sub>2</sub> yields a desilylated Cp'<sub>2</sub>Sm-imine-amido complex with a four-membered Sm(NSiMe<sub>3</sub>)(CPh)N=CHPh chelate ring (characterized by X-ray diffraction). Additional heating of this product under H<sub>2</sub> yields S<sub>6</sub>-symmetric (Cp'<sub>2</sub>SmCN)<sub>6</sub>, which contains an unusual chairlike 18-membered (SmCN)<sub>6</sub> ring (characterized by X-ray diffraction).

In contrast to the catalytic hydrogenation of olefins, far less is known about the equally exothermic hydrogenation of imines (e.g., eqs 1 and 2),<sup>1,2</sup> although the latter offers routes to a diverse



$$\Delta H = -32.6 \text{ kcal/mol}$$



$$\Delta H = -32.0 \text{ kcal/mol}$$

variety of amines, both achiral and chiral, natural and unnatural.<sup>3</sup> To date, the great majority of imine hydrogenation studies have employed late transition metal catalysts.<sup>1,3</sup> This is not surprising,

<sup>⊗</sup> Abstract published in *Advance ACS Abstracts*, April 1, 1997.

(1) (a) Bartok, M. *Stereochemistry of Heterogeneous Metal Catalysis*; Wiley: Chichester, 1985, pp 290–293. (b) Rylander, P. N. *Hydrogenation Methods*; Academic Press: New York, 1985, Chapter 7. (c) Tennant, G. In *Comprehensive Organic Chemistry*; Sutherland, O., Barton, D., Ollis, W. D., Eds.; Pergamon: Oxford, 1979; Vol. 2, pp 440–443.

(2) Heats of hydrogenation were computed using the AM1 Hamiltonian in the MOPAC molecular orbital package.

(3) For some recent examples of the homogeneous hydrogenation of imines and related substrates, see: (a) Hegedus, L. S. In *Comprehensive Organometallic Chemistry II*; Hegedus, L. S., Abel, E. W., Stone, F. G. A., Wilkinson, G., Eds.; Elsevier: Oxford, 1995; Vol. 12, pp 26–27 and references therein. (b) Noyori, R. *Asymmetric Catalysis in Organic Synthesis*; Wiley: New York, 1994; pp 82–85 and references therein. (c) Ball, G. E.; Cullen, W. R.; Fryzuk, M. D.; Henderson, W. J.; James, B. R.; MacFarlane, K. S. *Inorg. Chem.* **1994**, *33*, 1464–1468. (d) Bolm, C. *Angew. Chem., Int. Ed. Engl.* **1993**, *32*, 232–234. (e) Takaya, H.; Ohta, T.; Noyori, R. In *Catalytic Asymmetric Synthesis*; Ojima, I., Ed.; VCH Publishers: New York, 1993; Chapter 1 and references therein. (f) Burk, M. J.; Feaster, J. E. *J. Am. Chem. Soc.* **1992**, *114*, 626–627. (g) Becalski, A. G.; Cullen, W. R.; Fryzuk, M. D.; James, B. R.; Kang, G.-J.; Rettig, S. J. *Inorg. Chem.* **1991**, *30*, 5002–5008. (h) Spindler, F.; Pugin, B.; Blaser, H.-U. *Angew. Chem., Int. Ed. Engl.* **1990**, *29*, 558–559.

and metal–ligand bond enthalpy considerations<sup>4–6</sup> suggest, a priori, that the comparatively greater strength of early transition metal, d<sup>0</sup>,f-metal–heteroatom bonds might seriously impede the product-releasing hydrogenolysis step in many plausible homogeneous catalytic cycles. Hypothetical Scheme 1 illustrates this point for group 4 (only M = Zr thermochemical data are available), 4f, and 5f complexes,<sup>4–6</sup> where it can be seen that the M–N bond-forming step (i) is rather exothermic while the product-releasing M–N hydrogenolysis step (ii) is generally less so.

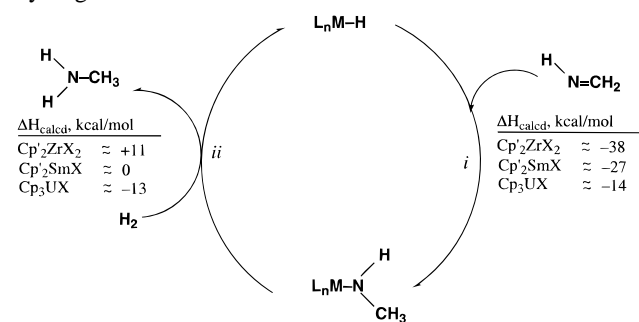
A striking example where early transition metal complexes are effective imine hydrogenation catalysts is the work of Buchwald and co-workers.<sup>7</sup> Here several classes of acyclic and cyclic imines are hydrogenated in moderate to high enantiomeric excess using a chiral ethylene-1,2-bis(tetrahydroindenyl)tita-

(4) The accuracy of these estimates is limited to some degree by the small current *D*(M–N) data base. Nevertheless, the Δ*H*<sub>calcd</sub> sums for Scheme 1, steps i and ii, are in reasonable agreement with the estimated Δ*H* for imine hydrogenation. Metal–ligand bond enthalpies are from the following: (a) Giardello, M. A.; King, W. A.; Nolan, S. P.; Porchia, M.; Sishta, C.; Marks, T. J. In *Energetics of Organometallic Species*; Martinho Simoes, J. A., Ed.; Kluwer: Dordrecht, The Netherlands, 1992; pp 35–54. (b) Nolan, S. P.; Stern, D.; Hedden, D.; Marks, T. J. *ACS Symp. Ser.* **1990**, *428*, 159–174. (c) Nolan, S. P.; Stern, D.; Marks, T. J. *J. Am. Chem. Soc.* **1989**, *111*, 7844–7853. (d) Schock, L. E.; Marks, T. J. *J. Am. Chem. Soc.* **1988**, *110*, 7701–7715. (e) Bruno, J. W.; Marks, T. J.; Morss, L. R. *J. Am. Chem. Soc.* **1983**, *105*, 6824–6832.

(5) Organic fragment bond enthalpies are from the following: (a) Giller, D.; Kanabus-Kaminska, J. M.; Maccoll, A. *J. Mol. Struct.* **1988**, *163*, 125–131. (b) McMillan, D. F.; Golden, D. M. *Annu. Rev. Phys. Chem.* **1982**, *33*, 493–532 and references therein. (c) Benson, S. W. *Thermochemical Kinetics*, 2nd ed.; John Wiley and Sons: New York, 1976; Appendix Tables A.10, A.11, and A.22. (d) Benson, S. W. *J. Chem. Educ.* **1965**, *42*, 502–518.

(6) Pedley, J. B.; Naylor, R. D.; Kirby, S. P. *Thermochemical Data of Organic Compounds*, 2nd ed.; Chapman and Hall: London, 1986; Appendix Tables 1 and 3.

(7) (a) Willoughby, C. A.; Buchwald, S. L. *J. Am. Chem. Soc.* **1994**, *116*, 11703–11714. (b) Willoughby, C. A.; Buchwald, S. L. *J. Am. Chem. Soc.* **1994**, *116*, 8952–8965. (c) Willoughby, C. A.; Buchwald, S. L. *J. Am. Chem. Soc.* **1992**, *114*, 7562–7564.

**Scheme 1.** Thermodynamics of Catalytic Imine Hydrogenation

nium(IV) binaphthalenediolate complex activated with *n*-BuLi + PhSiH<sub>3</sub>. Required pressures are rather high (80–2000 psi), turnover frequencies are modest ( $N_t \approx 0.5$ – $4.0 \text{ h}^{-1}$  at 65 °C), and added silane is required to stabilize the active species. The rate law ( $\nu \approx k[\text{Ti}]^1[\text{H}_2]^1[\text{imine}]^0$ ), lack of isotopic evidence for significant reversibility of imine insertion, and  $k(\text{H}_2)/k(\text{D}_2) = 1.5$  are in accord with Scheme 1, where step i is operationally irreversible under catalytic conditions and step ii not unexpectedly (vide supra) turnover-limiting. It was proposed that the active species is a d<sup>1</sup> Ti(III) complex (as opposed to the d<sup>0</sup> Ti(IV) of the precatalyst).<sup>7</sup>

Recent research in several laboratories has shown that lanthanocene complexes are highly active catalysts for olefin/acetylene transformations such as hydrogenation,<sup>8</sup> oligomerization/polymerization,<sup>9</sup> hydrosilylation,<sup>9c,10</sup> hydrophosphination,<sup>11</sup> hydroboration,<sup>12</sup> and ring-opening Ziegler polymerization.<sup>13</sup> With reference to organonitrogen transformations, these catalysts also mediate a variety of alkene and alkyne intramolecular and intermolecular hydroamination processes.<sup>14</sup> These characteristics, the general predictability/immobility of most lanthanide formal oxidation states, and thermochemical data<sup>4–6</sup> arguing that step ii of Scheme 1 is less endothermic for lanthanides suggest that organolanthanides might be competent and instructive imine hydrogenation catalysts. We report here a catalytic, synthetic, and molecular structure study of organolanthanide-mediated

imine hydrogenation, using well-defined precatalysts and focusing on scope, selectivity, mechanistic observations, and the informative nature of several unusual organolanthanide byproducts. Subsequent to our initial communication on this subject<sup>15</sup> and while this paper was being completed, the stoichiometric, aryl C–H activating reaction of  $(\text{Cp}'_2\text{SmH})_2$  ( $\text{Cp}' = \eta^5\text{-Me}_5\text{C}_5$ ) with 2-phenyl-1-pyrroline and several acyclic benzyldieneamines was communicated by Buchwald, Burns, et al.<sup>16</sup>

**Experimental Section**

**General Considerations.** All manipulations of air-sensitive materials were performed with the rigorous exclusion of oxygen and moisture in flame-dried Schlenk-type glassware on a dual manifold Schlenk line, interfaced to a high-vacuum ( $10^{-6}$  Torr) line, or in a nitrogen-filled Vacuum Atmospheres glovebox with a high-capacity recirculator (<1 ppm O<sub>2</sub>). Argon (Matheson, prepurified) and dihydrogen (Linde) were purified by passage through a MnO/SiO<sub>2</sub><sup>17</sup> oxygen-removal column and a Davison 4A molecular sieve column. Ether solvents (tetrahydrofuran, ethyl ether) were predried over KOH and distilled under nitrogen from sodium–benzophenone ketyl. Hydrocarbon solvents (toluene, pentane) were distilled under nitrogen from Na/K alloy. All solvents for vacuum line manipulations or catalytic experiments were stored *in vacuo* over Na/K alloy in resealable bulbs. Deuterated solvents were obtained from Cambridge Isotope Laboratories (all 99 atom % D) and were degassed and dried over Na/K alloy. Anhydrous lanthanide trichlorides were prepared from the corresponding sesquioxides Ln<sub>2</sub>O<sub>3</sub> (Cerac, Ln = La, Sm, Lu) and ammonium chloride.<sup>18</sup> The complexes  $\text{Cp}'_2\text{LaCH}(\text{TMS})_2$ ,<sup>9f</sup>  $\text{Cp}'_2\text{SmCH}(\text{TMS})_2$ ,<sup>9f</sup>  $\text{Cp}'_2\text{LuCH}(\text{TMS})_2$ ,<sup>9f</sup> and  $\text{Me}_2\text{SiCp}''_2\text{SmCH}(\text{TMS})_2$  ( $\text{Cp}'' = \eta^5\text{-Me}_4\text{Cp}$ )<sup>9e</sup> were synthesized according to published procedures. The solid lithium reagent  $\text{LiCH}(\text{SiMe}_3)_2$  was prepared according to literature methods.<sup>19</sup> Pentamethylcyclopentadiene was synthesized according to a procedure developed in this laboratory.<sup>20</sup> The imine substrates *N*-benzylidene(trimethylsilyl)amine (**2c**),<sup>21</sup> *N*-( $\alpha$ -methylbenzylidene)(methyl)amine (**2d**),<sup>22</sup> and *N*-( $\alpha$ -methylbenzylidene)-(benzyl)amine (**2e**)<sup>23</sup> were synthesized via modifications of literature methods. *N*-Benzylidene(methyl)amine (**2a**) and 2-methyl-1-pyrroline (**4**) were purchased from Aldrich and were distilled from BaO and LiAlH<sub>4</sub> and twice from freshly activated 4A molecular sieves. *N*-Benzylideneaniline (**2b**) was purchased from Aldrich and vacuum sublimed twice. Substrates **2c**, **3a**, and **3b** were distilled from BaO twice.

**Analytical Measurements.** NMR spectra were recorded on a Varian Gemini 300 (FT, 300 MHz, <sup>1</sup>H), VXR-300 (FT, 300 MHz, <sup>1</sup>H), or XL-400 (FT, 400 MHz, <sup>1</sup>H) instrument. <sup>1</sup>H and <sup>13</sup>C chemical shifts are

(8) (a) Haar, C. M.; Stern, C. L.; Marks, T. J. *Organometallics* **1996**, *15*, 1765–1784. (b) Giardello, M. A.; Conticello, V. P.; Brard, L.; Gagne, M. R.; Marks, T. J. *J. Am. Chem. Soc.* **1994**, *116*, 10241–10254. (c) Molander, G. A.; Hoberg, J. O. *J. Am. Chem. Soc.* **1992**, *114*, 3123–3125. (d) Molander, G. A.; Hoberg, J. O. *J. Org. Chem.* **1992**, *57*, 3266–3268. (e) Jeske, G.; Lauke, H.; Mauermann, H.; Schumann, H.; Marks, T. J. *J. Am. Chem. Soc.* **1985**, *107*, 8111–8118.

(9) (a) Mitchell, J. P.; Hajela, S.; Brookhart, S. K.; Hardcastle, K. I.; Henling, L. M.; Bercaw, J. E. *J. Am. Chem. Soc.* **1996**, *118*, 1045–1053. (b) Ihara, E.; Nodono, M.; Yasuda, H.; Kanehisa, N.; Kai, Y. *Macromol. Chem. Phys.* **1996**, *197*, 1909–1917. (c) Fu, P.-F.; Marks, T. J. *J. Am. Chem. Soc.* **1995**, *117*, 10747–10748. (d) Heeres, H. J.; Renkema, J.; Booi, M.; Meetsma, A.; Teuben, J. H. *Organometallics* **1988**, *7*, 2495–2502. (e) den Haan, K. H.; de Boer, J. L.; Teuben, J. H.; Spek, A. L.; Kajib-Prodic, B.; Hays, G. R.; Huis, R. *Organometallics* **1986**, *5*, 1726–1733. (f) Jeske, G.; Schock, L. E.; Swepton, P. N.; Schumann, H.; Marks, T. J. *J. Am. Chem. Soc.* **1985**, *107*, 8103–8110. (g) Jeske, G.; Lauke, H.; Mauermann, H.; Swepton, P. N.; Schumann, H.; Marks, T. J. *J. Am. Chem. Soc.* **1985**, *107*, 8091–8103. (h) Watson, P. L.; Parshall, G. W. *Acc. Chem. Res.* **1985**, *18*, 51–55.

(10) (a) Fu, P.-F.; Brard, L.; Li, Y.; Marks, T. J. *J. Am. Chem. Soc.* **1995**, *117*, 7157–7168. (b) Molander, G. A.; Nichols, P. J. *J. Am. Chem. Soc.* **1995**, *117*, 4415–4416. (c) Molander, G. A.; Julius, M. *J. Org. Chem.* **1992**, *57*, 6347–6351. (d) Sakakura, T.; Lautenschlager, H.; Tanaka, M. *J. Chem. Soc., Chem. Commun.* **1991**, 40–41.

(11) Giardello, M. A.; King, W. A.; Nolan, S. P.; Porchia, M.; Sishita, C.; Marks, T. J. In ref 4a, pp 35–51.

(12) (a) Harrison, K. N.; Marks, T. J. *J. Am. Chem. Soc.* **1992**, *114*, 9220–9221. (b) Bijpost, E. A.; Duchateau, R.; Teuden, J. H. *J. Mol. Catal.* **1995**, *95*, 121–128.

(13) (a) Jia, L.; Yang, X.; Seyam, A. M.; Albert, I. D. L.; Fu, P.-F.; Yang, S.; Marks, T. J. *J. Am. Chem. Soc.* **1996**, *118*, 7900–7913. (b) Yang, X.; Seyam, A. M.; Fu, P.-F.; Marks, T. J. *Macromolecules* **1994**, *27*, 4625–4626.

(14) (a) Li, Y.; Marks, T. J. *J. Am. Chem. Soc.* **1996**, *118*, 9295–9306. (b) Li, Y.; Marks, T. J. *Organometallics* **1996**, *15*, 3770–3772. (c) Li, Y.; Marks, T. J. *J. Am. Chem. Soc.* **1996**, *118*, 707–708. (d) Li, Y.; Fu, P.-F.; Marks, T. J. *Organometallics* **1994**, *13*, 439–440. (e) Giardello, M. A.; Conticello, V. P.; Brard, L.; Gagne, M. R.; Marks, T. J. *J. Am. Chem. Soc.* **1994**, *116*, 10241–10254. (f) Gagne, M. R.; Stern, C. L.; Marks, T. J. *J. Am. Chem. Soc.* **1992**, *114*, 275–294. (g) Gagne, M. R.; Brard, L.; Conticello, V. P.; Giardello, M. A.; Stern, C. L.; Marks, T. J. *Organometallics* **1992**, *11*, 2003–2005. (h) Gagne, M. R.; Nolan, S. P.; Marks, T. J. *Organometallics* **1990**, *9*, 1716–1718.

(15) Obora, Y.; Ohta, T.; Stern, C. L.; Marks, T. J. *Abstracts of Papers*, 211th National Meeting of the American Chemical Society, New Orleans, LA, March 1996; American Chemical Society: Washington, DC, 1996; INOR 129.

(16) Radu, N. S.; Buchwald, S. L.; Scott, B.; Burns, C. J. *Organometallics* **1996**, *15*, 3913–3915.

(17) (a) Moeseler, R.; Horvath, B.; Lindenau, D.; Horvath, E. G.; Krauss, H. L. *Z. Naturforsch.* **1976**, *31B*, 892–893. (b) McIlwrick, C. R.; Phillips, C. S. G. *J. Chem. Phys. E* **1973**, *6*, 1208–1210. (c) He, M.-Y.; Xiong, G.; Toscano, P. J.; Burwell, R. L., Jr.; Marks, T. J. *J. Am. Chem. Soc.* **1985**, *107*, 641–652.

(18) Meyer, G. *Inorg. Synth.* **1989**, *25*, 146–150.

(19) Cowley, A. H.; Kemp, R. A. *Synth. React. Inorg. Met.-Org. Chem.* **1981**, *11*, 591–595.

(20) Fendrick, C. M.; Schertz, L. D.; Mintz, E. A.; Marks, T. J. *Inorg. Synth.* **1992**, *29*, 193–197.

(21) Hart, D. J.; Kanai, K.; Thomas, D. G.; Yang, T.-K. *J. Org. Chem.* **1983**, *48*, 289–294.

(22) Evans, D. A.; Domeier, L. A. *Organic Syntheses*; Wiley: New York, 1988; Vol. VI, 818–820.

(23) In the Supplementary Material of ref 7c.

referenced to internal solvent resonances and reported relative to TMS. NMR experiments on air-sensitive samples were conducted in either Teflon valve-sealed tubes (J. Young) or in screw-capped tubes fitted with septa (Wilmad). IR spectra were recorded on a Mattson FT-IR spectrometer. MS studies were performed on a VG70-250 SE instrument with 70 eV electron impact ionization. We thank Dr. Doris Hung for assistance. Elemental analyses were performed by Oneida Research Services, Inc., Whitesboro, NY.

**Catalytic Hydrogenation Reactions.** A typical procedure is described for the high-pressure hydrogenation of **2a** using Cp<sub>2</sub>SmCH(TMS)<sub>2</sub> (**1b**) as the precatalyst. The quartz Griffin-Warden vessel (60 mL) and 500 mL dihydrogen reservoir described previously<sup>24</sup> were employed in these experiments. In the glovebox, a solution of Cp<sub>2</sub>SmCH(TMS)<sub>2</sub> (**1b**; 58 mg, 0.10 mmol) in toluene (2.0 mL) and **2a** (1.18 g, 10.0 mmol) were placed in the dry (flamed under vacuum) quartz vessel. The closed vessel was then removed from the glovebox and connected to the high-vacuum line, and the solution was degassed by three freeze-pump-thaw cycles. To this mixture was then added pressurized Matheson UHP H<sub>2</sub> (190 psi), and the reaction mixture was rapidly stirred at 90 °C. The progress of the reaction was monitored by the drop in H<sub>2</sub> pressure, and runs were typically terminated (by venting) after 96 h or when the pressure no longer decreased. Analysis of the rather concentrated reaction mixture by <sup>1</sup>H NMR was straightforward and indicated only the presence of **2a** (8%) and of the hydrogenation product, *N*-benzylmethylamine (92%). All hydrogenation products were identified by comparison to literature <sup>1</sup>H NMR spectra.<sup>25</sup> NMR scale reactions were carried out in NMR tubes equipped with Teflon J. Young valves. Sample charging was similar to that described above, and H<sub>2</sub> pressures were on the order of 20 psi. Sample tubes were regularly shaken during hydrogenation studies.

**NMR Study of the Reaction of Cp<sub>2</sub>SmCH(TMS)<sub>2</sub> with *N*-Benzylidene(methyl)amine (**2a**). Synthesis of **4a** and **4b**.** A 5 mm NMR tube equipped with a Teflon valve was charged in the glovebox with Cp<sub>2</sub>SmCH(TMS)<sub>2</sub> (20 mg, 0.050 mmol), **2a** (21 mg, 0.18 mmol), and C<sub>6</sub>D<sub>6</sub> (1.0 mL). The tube was then sealed, and the reaction was monitored by NMR at room temperature over a period of 136 h. After this time, the tube was pressurized with H<sub>2</sub> (ca. 20 psi). After 22 h at room temperature, the tube was then heated at 90 °C for 120 h. From the NMR spectra, two new samarium complexes (**4a**, **4b**) could be detected. Formation of complexes **4a** and **4b** was further confirmed by GC/MS analysis of the organic products formed upon D<sub>2</sub>O quenching of this reaction mixture (**5a**, **5b**).

**Data for 4a.** <sup>1</sup>H NMR (C<sub>6</sub>D<sub>6</sub>): δ -7.30 (s, 3H, Me), 1.30 (s, 30H, C<sub>5</sub>(CH<sub>3</sub>)<sub>5</sub>), 6.45 (br d, 1H), 6.80 (br s, 1H), 7.20 (t, 1H), 8.00 (t, 1H), 8.60 (d, 1H). D<sub>2</sub>O-quenched organic product (**5a**) <sup>1</sup>H NMR (C<sub>6</sub>D<sub>6</sub>): δ 3.40 (s, 3H), 7.0-7.9 (5H). MS (EI, 70 eV, relative intensity): *m/e* 120 (M<sup>+</sup>, 100), 91 (53), 77 (22), 65 (27).

**Data for 4b.** <sup>1</sup>H NMR (C<sub>6</sub>D<sub>6</sub>): δ -13.3 (s, 3H, Me), -10.6 (s, 3H, Me), 1.20 (s, 30H, C<sub>5</sub>(CH<sub>3</sub>)<sub>5</sub>), 6.80 (d, 1H), 7.00 (t, 2H), 7.0-7.2 (2H, m), 7.60 (d, 2H), 7.90 (d, 1H), 8.40 (br s, 2H), 11.8 (very br s, 1H). D<sub>2</sub>O-quenched organic product (**5b**) <sup>1</sup>H NMR (C<sub>6</sub>D<sub>6</sub>): δ 2.40 (s, 3H), 3.20 (s, 3H), 3.40 (s, 1H), 7.0-7.9 (m, 9H). MS (EI, 70 eV, relative intensity): *m/e* 224 (M<sup>+</sup> - CH<sub>3</sub>, 60), 120 (14), 105 (100), 91 (16), 77 (40), 51 (12).

**Synthesis of Cp<sub>2</sub>Sm(C<sub>10</sub>H<sub>18</sub>N<sub>2</sub>) (**6**).** For an NMR scale experiment, a 5 mm NMR tube with a Teflon valve (previously flamed *in vacuo*) was charged in the glovebox with Cp<sub>2</sub>SmCH(TMS)<sub>2</sub> (29 mg, 0.050 mmol), 2-methyl-1-pyrroline (**2f**; 12 mg, 0.15 mmol), and toluene-*d*<sub>8</sub> (1.0 mL). The tube was then pressurized with H<sub>2</sub> (ca. 20 psi). After 12 h, the title compound **7** was detected in 88% yield. For a preparative scale synthesis, a 20 mL J. Young valve equipped storage tube was loaded in the glovebox with Cp<sub>2</sub>SmCH(TMS)<sub>2</sub> (100 mg, 0.17 mmol), 2-methyl-1-pyrroline (42 mg, 0.50 mmol), and toluene (2 mL). After

2 days, the solvent was removed *in vacuo*, and the product **6** was obtained by recrystallization from pentane (-78 °C) as an orange solid. Yield: 51 mg (50%). <sup>1</sup>H NMR (toluene-*d*<sub>8</sub>): δ -18.5 (br s, 1H), -15.9 (br s, 1H), -11.8 (br s, 1H), -9.0 (br s, 1H), -3.60 (br s, 1H), -2.90 (br s, 1H), 1.18 (s, 15H), 1.30 (s, 15H), 1.35-1.45 (m, 3H), 1.5-1.7 (m, 1H), 3.52 (ddd, 1H, *J* = 6, 9, 12 Hz), 4.92 (ddd, 1H, *J* = 6, 11, 11 Hz), 5.6 (s, 3H), 5.65 (d, 1H, *J* = 15 Hz), 10.9 (br, 1H). MS (EI, 70 eV, relative intensity): *m/e* 588 (M<sup>+</sup>(<sup>152</sup>Sm), 2), 583 (M<sup>+</sup>(<sup>147</sup>Sm), 1), 573 (M<sup>+</sup>(<sup>152</sup>Sm) - CH<sub>3</sub>, 8), 571 (M<sup>+</sup>(<sup>150</sup>Sm) - CH<sub>3</sub>, 4), 568 (M<sup>+</sup>(<sup>147</sup>Sm) - CH<sub>3</sub>, 5), 513 (10), 512 (4), 511 (12), 509 (7), 508 (8), 507 (8), 506 (6), 455 (12), 454 (6), 453 (13), 451 (6), 450 (9), 449 (8), 448 (7), 441 (19), 439 (27), 438 (100), 437 (10), 436 (48), 435 (71), 434 (66), 433 (72), 430 (15), 424 (16), 423 (15), 422 (18), 421 (14), 419 (12), 418 (16), 417 (14), 416 (10), 413 (7), 412 (8), 410 (7), 399 (11), 397 (13). HRMS (EI, 70 eV): *m/e* calcd for C<sub>29</sub>H<sub>45</sub>N<sub>2</sub><sup>147</sup>Sm (M<sup>+</sup> - CH<sub>3</sub>) 568.2732, found 568.2712.

**Preparation of Cp<sub>2</sub>Sm(C<sub>17</sub>H<sub>21</sub>NSi) (**7**).** For an NMR scale experiment, a 5 mm NMR tube with a Teflon valve (previously flamed *in vacuo*) was charged in the glovebox with Cp<sub>2</sub>SmCH(TMS)<sub>2</sub> (29 mg, 0.050 mmol), *N*-benzylidene(trimethylsilyl)amine (**2c**; 71 mg, 0.40 mmol), and C<sub>6</sub>D<sub>6</sub> (1 mL). The tube was then pressurized with H<sub>2</sub> (ca. 20 psi). Subsequent concentration of this mixture to 0.3 mL and standing at room temperature overnight afforded yellow crystals of **7**. For a preparative scale synthesis, a 20 mL J. Young valve equipped storage tube was loaded in a glovebox with Cp<sub>2</sub>SmCH(TMS)<sub>2</sub> (100 mg, 0.17 mmol), *N*-benzylidene(trimethylsilyl)amine (71 mg, 0.40 mmol), and toluene (2.0 mL). The mixture was then placed under a H<sub>2</sub> atmosphere. After 2 days, solvent was removed *in vacuo*, and the product was obtained by recrystallization from pentane (-78 °C) as a yellow solid. Yield: 55 mg (44%). <sup>1</sup>H NMR (C<sub>6</sub>D<sub>6</sub>): δ -9.90 (br s, 2H, ortho of Ph(1)), -3.40 (br s, 9H, Si(CH<sub>3</sub>)<sub>3</sub>), 1.3 (s, 15H, C<sub>5</sub>(CH<sub>3</sub>)<sub>5</sub>), 1.50 (s, 15H, C<sub>5</sub>(CH<sub>3</sub>)<sub>5</sub>), 2.60 (br s, 1H), 3.60 (t, 2H, meta of Ph(1)), 4.60 (t, 1H, para of Ph(1)), 8.00 (t, 1H, para of Ph(2)), 8.40 (t, 2H, meta of Ph(2)), 11.5 (br s, 2H, ortho of Ph(2)), and 13.15 (s, 1H); MS (EI, 70 eV, relative intensity): *m/e* 633 (M<sup>+</sup>(<sup>152</sup>Sm) - (CH<sub>3</sub>)<sub>3</sub>Si, 5), 631 (M<sup>+</sup>(<sup>150</sup>Sm) - (CH<sub>3</sub>)<sub>3</sub>Si, 6), 628 (M<sup>+</sup>(<sup>147</sup>Sm) - (CH<sub>3</sub>)<sub>3</sub>Si, 4), 500 (6), 499 (34), 498 (90), 497 (39), 496 (100), 495 (17), 494 (52), 493 (71), 492 (64), 491 (62), 489 (6), 488 (17), 363 (24), 362 (5), 361 (28), 359 (12), 358 (18), 357 (16), 356 (17). Anal. Calcd for C<sub>37</sub>H<sub>51</sub>N<sub>2</sub>SiSm: C, 63.28; H, 7.32; N, 3.99. Found: C, 62.54; H, 7.15; N, 3.58.

**Synthesis of [Cp<sub>2</sub>SmCN]<sub>6</sub> (**8**).** A mixture of Cp<sub>2</sub>SmCH(TMS)<sub>2</sub> (29 mg, 0.05 mmol) and *N*-benzylidene(trimethylsilyl)amine (**2c**; 53 mg, 0.30 mmol) in C<sub>6</sub>D<sub>6</sub> (1.0 mL) was heated at 90 °C for 1 week under H<sub>2</sub> (ca. 20 psi of pressure) in a 5 mm NMR tube with a Teflon valve. During heating, orange crystals were observed to grow. The mother liquor was next removed by decantation, the crystals were dried *in vacuo*, and degassed Paratone N (Exxon) was poured over the crystals for diffraction analysis (see below). A preparative scale synthesis was carried out in a manner similar to that of the NMR reaction with Cp<sub>2</sub>SmCH(TMS)<sub>2</sub> (100 mg, 0.17 mmol) and *N*-benzylidene(trimethylsilyl)amine (140 mg, 0.80 mmol) in C<sub>6</sub>D<sub>6</sub> (2 mL) under 20 psi of H<sub>2</sub> at 90 °C. Solid **8** did not crystallize during heating; however, analytically pure product (10-15 mg) could be obtained by crystallization from toluene (-78 °C). <sup>1</sup>H NMR (C<sub>6</sub>D<sub>6</sub>): δ 1.68 (s, 60H), 1.82 (s, 60H). MS (EI, 70 eV, relative intensity): *m/e* 315 ([Cp<sup>152</sup>SmCN]<sup>+</sup>, 4), 313 ([Cp<sup>150</sup>SmCN]<sup>+</sup>, 6), 298 (8), 296 (11), 287 (5), 285 (5), 267 (8), 265 (5), 240 (22), 193 (33), 150 (76), 149 (72), 135 (100). IR (Nujol mull): 2980-2850 s, 2360 m, 2332 m, 1458 s, 1243 w, 1150 w, 1088 m, 936 m, 840 w, 722 m cm<sup>-1</sup>. Anal. Calcd for C<sub>126</sub>H<sub>180</sub>N<sub>6</sub>Sm<sub>6</sub>: C, 56.44; H, 6.77; N, 3.13. Found: C, 56.57; H, 7.38; N, 3.00.

**Synthesis of Cp<sub>2</sub>La(C<sub>13</sub>H<sub>12</sub>N) (**10**).** For an NMR scale experiment, a 5 mm NMR tube with a Teflon valve (previously flamed *in vacuo*) was charged with Cp<sub>2</sub>LaCH(TMS)<sub>2</sub> (17 mg, 0.030 mmol), *N*-benzylidene(trimethylsilyl)amine (**2c**; 5 mg, 0.03 mmol), and C<sub>6</sub>D<sub>6</sub> (1.0 mL). After 1 day, no reaction was detectable. H<sub>2</sub> (20 psi) was then added to this mixture. Immediately, the lemon-yellow color changed to orange. The Cp<sub>2</sub>LaCH(TMS)<sub>2</sub> was no longer visible in the <sup>1</sup>H NMR, and a new complex (**10**) was detected in ~60% yield. For a preparative scale synthesis, a 20 mL J. Young valve equipped storage tube was loaded in the glovebox with Cp<sub>2</sub>LaCH(TMS)<sub>2</sub> (100 mg, 0.18 mmol), **2c** (33 mg, 0.18 mmol), and toluene (2.0 mL). The reaction mixture was then placed under a H<sub>2</sub> atmosphere. After 1 week, the solvent

(24) Eisen, M. S.; Marks, T. J. *J. Am. Chem. Soc.* **1992**, *114*, 10358-10368.

(25) (a) **3a**: Bernatis, P.; Laurie, J. C. V.; Dubois, M. R. *Organometallics* **1990**, *9*, 1607-1617. (b) **3b**: Hayashi, T.; Abe, F.; Sakakura, T.; Tanaka, M. *J. Mol. Catal.* **1990**, *58*, 165-170. (c) **3c**: Narula, S. P.; Kapur, N. *Inorg. Chim. Acta* **1983**, *73*, 183-187. (d) **3d**: Whitesides, G. M.; Lewis, D. W. *J. Am. Chem. Soc.* **1971**, *93*, 5914-5916. (e) **3e**: Bakos, J.; Orosz, A.; Heil, B.; Laghari, M.; Lhoste, P.; Sinou, D. *J. Chem. Soc., Chem. Commun.* **1991**, 1684-1685. (f) **3f**: Gagne, M. R.; Nolan, S. P.; Marks, T. J. *Organometallics* **1990**, *9*, 1716-1718.

**Table 1.** Summary of Crystal Structure Data for Complexes **6**, **7**, and **8**<sup>a</sup>

complex	<b>6</b>	<b>7</b>	<b>8</b>
formula	SmC <sub>30</sub> H <sub>48</sub> N <sub>2</sub>	SmC <sub>37</sub> H <sub>52</sub> N <sub>2</sub> Si	Sm <sub>6</sub> C <sub>126</sub> H <sub>180</sub> N <sub>6</sub>
crystal system	monoclinic	monoclinic	hexagonal
space group	<i>P</i> <sub>2</sub> <sub>1</sub> / <i>n</i> (no. 14)	<i>P</i> <sub>2</sub> <sub>1</sub> / <i>n</i> (no. 14)	<i>R</i> 3( <i>h</i> ) (no. 148)
<i>a</i> , Å	10.517(2)	14.064(4)	31.310(7)
<i>b</i> , Å	17.243(2)	14.668(2)	
<i>c</i> , Å	15.227(3)	16.801(6)	10.873(2)
$\beta$ (deg)	93.90(2)	92.44(2)	
<i>V</i> , Å <sup>3</sup>	2755	3462	9231(6)
$\bar{Z}$	4	4	18
<i>d</i> (calcd), g/cm <sup>3</sup>	1.413	1.349	1.486
crystal size, mm	0.48 × 0.31 × 0.08	0.22 × 0.13 × 0.06	0.35 × 0.30 × 0.08
color, habit	orange, platy	yellow, platy	yellow, platy
$\mu$ , cm <sup>-1</sup>	21.58	17.60	28.75
scan type	$\omega$ - $\theta$	$\omega$ - $\theta$	$\omega$ - $\theta$
transmission factors range	0.54–0.84	0.71–0.88	0.66–0.87
$2\theta$ range, deg	2.0–46	2.0–47.9	2.0–46
intensities (unique, <i>R</i> <sub>i</sub> )	4150 (3982, 0.026)	5887 (5675, 0.087)	5889 (2854, 0.071)
intensities > 3.00 $\sigma$ ( <i>I</i> )	3244	2959	2235
number of parameters	299	371	207
<i>R</i>	0.027	0.039	0.038
<i>R</i> <sub>w</sub>	0.035	0.037	0.047
GOF	1.65	1.51	1.86
max shift/error in final cycle	0.01	0.00	0.01

<sup>a</sup> Diffractometer, Enraf-Nonius, CAD4; temperature for data collection, -120 °C; radiation, graphite monochromator, Mo K $\alpha$ ,  $\lambda$  = 0.710 69.

was removed under high vacuum, and pentane (2 mL) was added. The product **10** was obtained by recrystallization from pentane at -78 °C as a yellow solid. Yield: 34 mg (33%). <sup>1</sup>H NMR (C<sub>6</sub>D<sub>6</sub>):  $\delta$  1.80 (s, 30H), 4.25 (s, 2H), 6.25 (br s, 2H), 6.90 (t, 2H, *J* = 7.0 Hz), 7.0–7.2 (m, 6H). MS (EI, 70 eV, relative intensity): *m/e* 591 (M<sup>+</sup>, 8) 457 (24), 456 (100), 425 (19), 410 (20), 409 (98), 408 (18), 282 (12), 273 (46). HRMS (EI, 70 eV): *m/e* calcd for C<sub>33</sub>H<sub>42</sub>NLa 591.2381, found 591.2414. Anal. Calcd for C<sub>33</sub>H<sub>42</sub>NLa: C, 67.00; H, 7.16; N, 2.37. Found: C, 66.42; H, 7.26; N, 2.42.

**Synthesis of Cp<sup>+</sup>Sm(C<sub>13</sub>H<sub>12</sub>N) (11).** For an NMR scale experiment, a 5 mm NMR tube with a Teflon valve (previously flamed *in vacuo*) was charged in the glovebox with Cp<sup>+</sup>SmCH(TMS)<sub>2</sub> (35 mg, 0.060 mmol), *N*-benzylidene(trimethylsilyl)amine (**2c**; 21 mg, 0.12 mmol), and C<sub>6</sub>D<sub>6</sub> (1.0 mL). After 3 h, no reaction was detectable. H<sub>2</sub> (ca. 20 psi) was then added to this mixture. Immediately the color changed to dark red, and then to orange. The <sup>1</sup>H NMR revealed that the Cp<sup>+</sup>SmCH(TMS)<sub>2</sub> was consumed, and a new complex (**11**) formed in quantitative yield. For a preparative scale synthesis, a 20 mL J. Young valve equipped storage tube was loaded in the glovebox with Cp<sup>+</sup>SmCH(TMS)<sub>2</sub> (100 mg, 0.17 mmol), **2c** (72 mg, 0.40 mmol), and toluene (2.0 mL). The tube was then placed under a H<sub>2</sub> atmosphere. After 1 week, the solvent was removed *in vacuo* and pentane (2.0 mL) added. The product **11** was obtained by recrystallization from pentane at -78 °C as a red solid. Yield: 51 mg (49%). <sup>1</sup>H NMR (C<sub>6</sub>D<sub>6</sub>):  $\delta$  -32.0 (br s, 1H), -2.20 (br s, 1H), -0.42 (s, 30H), 2.75 (br d, 2H, *J* = 7.4 Hz, ortho of Ph), 2.95 (br s, 2H), 5.05 (t, 1H, *J* = 8.3 Hz), 5.30 (t, 2H, *J* = 7.4 Hz, meta of Ph), 5.98 (t, 1H, *J* = 7.4 Hz, para of Ph), 7.00 (m, 1H), and 11.0 (br s, 1H). MS (EI, 70 eV, relative intensity): *m/e* 604 (M<sup>+</sup>(<sup>152</sup>Sm), 11), 602 (M<sup>+</sup>(<sup>150</sup>Sm), 5), 599 (M<sup>+</sup>(<sup>147</sup>Sm), 6), 472 (20), 471 (45), 470 (24), 469 (51), 468 (9), 467 (30), 466 (38), 465 (36), 464 (29), 463 (3), 462 (4), 461 (6), 441 (8), 440 (37), 439 (9), 438 (44), 437 (3), 436 (18), 435 (27), 434 (24), 425 (20), 424 (88), 423 (25), 422 (100), 421 (8), 420 (44), 419 (67), 418 (59), 417 (61), 415 (3), 414 (12). HRMS (EI, 70 eV): *m/e* calcd for C<sub>33</sub>H<sub>42</sub>N<sup>147</sup>Sm 599.2466, found 599.2456. Anal. Calcd for C<sub>33</sub>H<sub>42</sub>N<sup>147</sup>Sm: C, 65.72; H, 7.02; N, 2.32. Found: C, 65.77; H, 6.97; N, 2.28.

**X-ray Crystallographic Studies of Complexes 6, 7, and 8.** Suitable crystals of **6**, **7**, and **8** for diffraction studies were grown by slow cooling of a pentane/toluene solution of each complex at -25 °C. In each case, the solvent was decanted and Paratone N (Exxon, dried and degassed at 120 °C, 10<sup>-6</sup> Torr, for 24 h) was poured over the crystals in the glovebox. The crystals were mounted on glass fibers and transferred to the cold stream (-120 °C) of the Enraf-Nonius CAD4 diffractometer. Final cell dimensions were obtained by least-squares fits to the automatically centered settings for 25 reflections. Three reference reflections monitored during data collection for each crystal

showed no significant variations. Intensity data were all corrected for absorption, anomalous dispersion and Lorentz and polarization effects.<sup>26</sup> The space group choice for each complex was unambiguously determined. Unit cell and data collection parameters are summarized in Table 1.

Subsequent computations were carried out on a SGI Indy computer. The structure of complex **6** was solved by direct methods (SHELXS-86).<sup>27</sup> The non-hydrogen atoms were refined anisotropically. Hydrogen atoms were fixed in idealized positions. The maximum peak on the final difference Fourier map (0.90 e<sup>-</sup> Å<sup>-3</sup>) was located in the vicinity of the Sm positions. Neutral atom scattering factors were taken from Cromer and Waber.<sup>28</sup> Anomalous dispersion effects were included in *F*<sub>calc</sub>,<sup>29</sup> the values for  $\Delta f'$  and  $\Delta f''$  were those of Cromer.<sup>30</sup> The structure of **7** was solved with SHELX-86 and expanded using Fourier techniques.<sup>31</sup> The non-hydrogen atoms were refined, and hydrogen atoms were fixed in idealized positions. The maximum peak on the final difference Fourier map (0.95 e<sup>-</sup> Å<sup>-3</sup>) was located in the vicinity of the Sm position. Neutral atom scattering factors were taken from Cromer and Waber.<sup>28</sup> Anomalous dispersion effects were included in *F*<sub>calc</sub>,<sup>29</sup> and the values for  $\Delta f'$  and  $\Delta f''$  were those of Creagh and McAuley.<sup>32</sup> The values for the mass attenuation coefficients were those of Creagh and Hubbel.<sup>33</sup> The structure of **8** was solved using a Patterson map (SHELXS-86).<sup>27</sup> The non-hydrogen atoms were refined anisotropically, and hydrogen atoms were fixed in idealized positions. The space group for **8** is not unambiguously determined. The assignment is based on successful solution and refinement of the proposed model and statistical analysis of the intensity distribution. The disordered C–N bonds were refined using group isotropic thermal parameters with N1(CN1)–C02(CN2) refined to an occupancy of 0.494

(26) Cromer, D. T.; Waber, J. T. *International Tables for X-Ray Crystallography*; The Kynoch Press: Birmingham, England, 1974; Vol. IV, pp 149–150.

(27) Sheldrick, G. M. In *Crystallographic Computation*; Sheldrick, G. M., Kruger, C., Goddard, R., Eds.; Oxford University Press: Oxford, 1985; pp 175–189.

(28) Reference 26, Vol. IV, Table 2.2A.

(29) Ibers, J. A.; Hamilton, W. C. *Acta Crystallogr.* **1964**, *17*, 781.

(30) Reference 26, Vol. IV, Table 2.3.1.

(31) DIRDIF92: Beurskens, P. T.; Admiraal, G.; Beurskens, G.; Bosman, W. P.; Garcia-Granda, S.; Gould, R. O.; Smits, J. M. M.; Smykalla, C. The DIRDIF program system, Technical Report of the Crystallography Laboratory, University of Nijmegen, The Netherlands, 1992.

(32) Creagh, D. C.; McAuley, W. J. In *International Tables for Crystallography*; Wilson, A. J. C., Ed.; Kluwer Academic Publishers: Boston, 1992; Vol. C, Table 4.2.6.8, pp 219–222.

(33) Creagh, D. C.; Hubbel, J. H. In *International Tables for Crystallography*; Wilson, A. J. C., Ed.; Kluwer Academic Publishers: Boston, 1992; Vol. C, Table 4.2.4.3, pp 200–206.

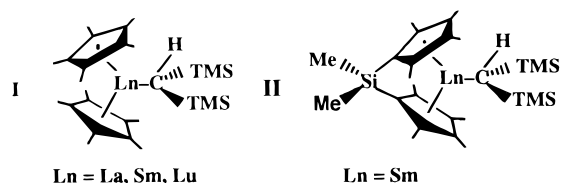
and N<sub>2</sub>(CN)<sub>2</sub>–C01(CN<sub>1</sub>) refined to an occupancy of 0.506. The maximum peak in the final difference Fourier map (1.42 e<sup>-</sup> Å<sup>-3</sup>) was located in the vicinity of the Sm position. Neutral atom scattering factors were taken from Cromer and Waber.<sup>28</sup> Anomalous dispersion effects were included in  $F_{\text{calc}}$ ,<sup>29</sup> and the values for  $\Delta f'$  and  $\Delta f''$  were those of Cromer.<sup>30</sup>

All calculations were performed using the TEXSAN<sup>34</sup> crystallographic software package of Molecular Structure Corp.

## Results

This section begins with a discussion of organolanthanide + imine catalytic hydrogenation phenomenology, focusing on the influence of imine structure and substituents, organolanthanide metal and ancillary ligation, added silanes, and reaction conditions on the hydrogenation process. In several cases, informative organolanthanide + substrate reaction products were detected in the hydrogenation studies and were then pursued in stoichiometric syntheses, followed by further spectroscopic and diffractometric characterization. The resulting picture both expands the scope and reveals some of the thermodynamic sinks prevalent in this type of catalytic chemistry.

**Organolanthanide-Catalyzed Imine Hydrogenation.** Homogeneous imine hydrogenation experiments using a variety of substrates, precatalysts (Cp'<sub>2</sub>LnCH(TMS)<sub>2</sub>, **I**; Me<sub>2</sub>SiCp'<sub>2</sub>-LnCH(TMS)<sub>2</sub>, **II**), and reaction conditions (typically substrate:



catalyst = 100:1) were carried out in toluene solution with rigorous exclusion of oxygen and moisture.<sup>8a,b,24</sup> Both NMR scale (20 psi of UHP H<sub>2</sub>) and preparative scale (190 psi of UHP H<sub>2</sub>) reactions were performed (see the Experimental Section for details). Since relatively concentrated solutions were employed, NMR spectroscopy of the reaction mixtures provided an effective and convenient analytical technique. Results are compiled in Table 2. It was found that acyclic imines undergo far more rapid hydrogenation than cyclic imines, with the latter giving trace (entries 14 and 15) to negligible yields of hydrogenation products. The acyclic imines undergo regiospecific hydrogenation to form known products<sup>25</sup> (identified by <sup>1</sup>H NMR) at modest turnover frequencies. Although few direct comparisons are available, the 2e → 3e (entry 13) reduction with  $N_t \approx 0.70 \text{ h}^{-1}$  at 90 °C, 190 psi of H<sub>2</sub>, compares favorably with the titanocene-mediated reduction ( $N_t \approx 2.0 \text{ h}^{-1}$  at 65 °C, 2000 psi of H<sub>2</sub>).<sup>7b</sup> Using the equipment described previously<sup>24</sup> and under conditions which were approximately zero-order in H<sub>2</sub> pressure, the rate of H<sub>2</sub> uptake in a high-pressure organo-samarium-catalyzed reduction of *N*-benzylidene(methyl)amine (Table 2, entry 1) was monitored as a function of time. At 90 °C, the uptake is approximately linear (Figure 1) to  $\geq 85\%$  conversion. These results are consistent with a catalytic rate law which is initially zero-order in imine, although deviations are evident at high conversion and may reflect some catalyst deactivation (vide infra). Not surprisingly, hydrogenation rates are greater at higher temperatures (entries 1, 3, and 4) and at higher H<sub>2</sub> pressures (comparisons to 20 psi NMR experiments).

In regard to imine substituents, both *N*-aryl and *N*-SiMe<sub>3</sub> substituents are deactivating with respect to hydrogenation (entries 9 and 11 vs entry 1), as is imine *C*-methyl substitution

**Table 2.** Hydrogenation of Imines Catalyzed by Organolanthanide Complexes<sup>a</sup>

entry	imine	amine	precatalyst	H <sub>2</sub> /psi	Time/h	N <sub>t</sub> /h <sup>-1</sup> (°C)	Conv/ % <sup>b</sup>
1.			Cp' <sub>2</sub> SmR <sup>d</sup>	190	92	1.0 (90)	92
			Cp' <sub>2</sub> SmR + PhSiH <sub>3</sub>	190	44	2.2 (90)	98
3.			Cp' <sub>2</sub> SmR	190	122	0.50 (50)	57
4.			Cp' <sub>2</sub> SmR	200	51	0.04 (25)	4
5.			Cp' <sub>2</sub> LaR	140	50	0.05 (25)	11
6.			Cp' <sub>2</sub> LaR <sup>d</sup>	190	75	0.03 (50)	5
7.			Cp' <sub>2</sub> LuR <sup>d</sup>	190	92	0.60 (90)	51
8.			SiSmR <sup>d</sup>	190	93	– (90)	trace
9.			Cp' <sub>2</sub> SmR	190	120	0.10 (90)	16
			Cp' <sub>2</sub> SmR + PhSiH <sub>3</sub>	190	120	– (90)	10 <sup>f</sup>
11.			Cp' <sub>2</sub> SmR	190	58	0.40 (90)	21
12.			Cp' <sub>2</sub> SmR	190	144	0.20 (90)	26
13. <sup>c</sup>			Cp' <sub>2</sub> SmR	190	134	0.70 (90)	98
			+ PhSiH <sub>3</sub>				
14. <sup>g</sup>			Cp' <sub>2</sub> SmR	190	106	– (90)	trace
			+ PhSiH <sub>3</sub>	190	89	– (90)	trace
15.			Cp' <sub>2</sub> LaR	190	89	– (90)	trace

<sup>a</sup> Solution of substrate (4–5 mol/L) and catalyst (~100:1) in toluene stirred under H<sub>2</sub> pressure. <sup>b</sup> Conversion determined by <sup>1</sup>H NMR analysis. <sup>c</sup> Reaction carried out in the presence of PhSiH<sub>3</sub> (PhSiH<sub>3</sub>:catalyst = 3.6). <sup>d</sup> Cp'<sub>2</sub>SmR = (η<sup>5</sup>-Me<sub>5</sub>C<sub>5</sub>)<sub>2</sub>SmCH(SiMe<sub>3</sub>)<sub>2</sub>; Cp'<sub>2</sub>LaR = (η<sup>5</sup>-Me<sub>5</sub>C<sub>5</sub>)<sub>2</sub>LaCH(SiMe<sub>3</sub>)<sub>2</sub>; Cp'<sub>2</sub>LuR = (η<sup>5</sup>-Me<sub>5</sub>C<sub>5</sub>)<sub>2</sub>LuCH(SiMe<sub>3</sub>)<sub>2</sub>; SiSmR = Me<sub>2</sub>Si(η<sup>5</sup>-Me<sub>4</sub>C<sub>5</sub>)SmCH(SiMe<sub>3</sub>)<sub>2</sub>. <sup>e</sup> Reaction carried out in the presence of PhSiH<sub>3</sub> (PhSiH<sub>3</sub>:catalyst = 10). <sup>f</sup> Hydrosilylation product obtained in 10% yield. <sup>g</sup> Reaction carried out in the presence of PhSiH<sub>3</sub> (PhSiH<sub>3</sub>:catalyst = 30).

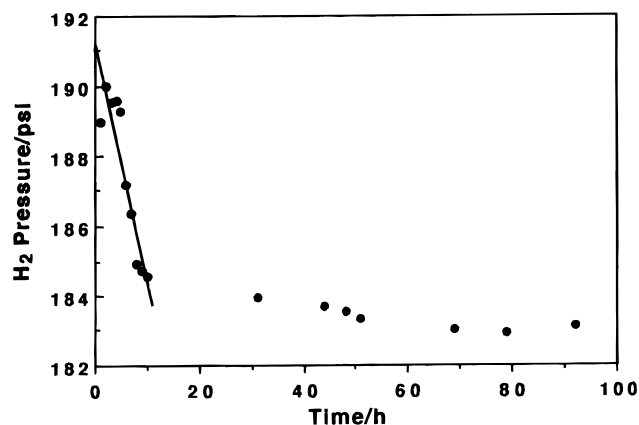
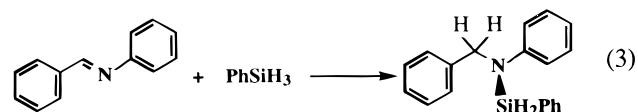


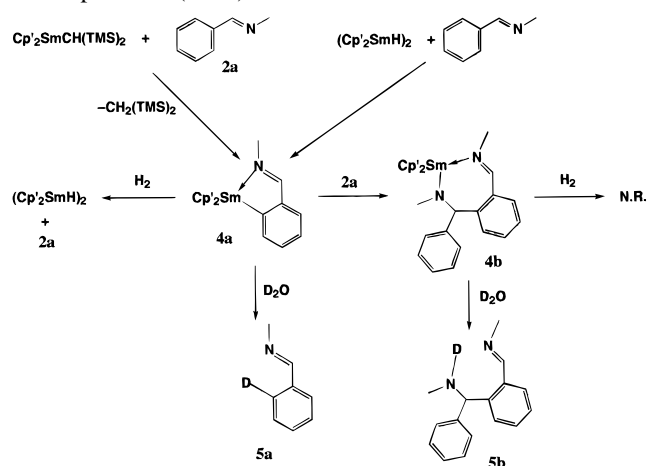
**Figure 1.** Time dependence of the reactor H<sub>2</sub> pressure in the hydrogenation of *N*-benzylidene(methyl)amine (**2a**) using Cp'<sub>2</sub>SmCH(SiMe<sub>3</sub>)<sub>2</sub> as the precatalyst at 90 °C. The line represents a least-squares fit to the initial data points. Fits of the data to first-order behavior were less convincing.

(entry 12 vs entry 1). As in the case of titanocene-mediated reduction, PhSiH<sub>3</sub> has a modest accelerating effect (entry 1 vs entry 2); however, in the case of *N*-benzylideneaniline (**2b**), a hydrosilylation product is detected in ca. 10% yield (eq 3).<sup>35</sup>



Interestingly and in marked contrast to metal and ancillary ligand sensitivities evident in a variety of organolanthanide-catalyzed-

(34) TEXSAN Structure Solution Package; Molecular Structure Corp.: The Woodlands, 1985 and 1992.

**Scheme 2.** Reaction of *N*-Benzyldene(methyl)amine (**2a**) with  $\text{Cp}'_2\text{SmCH}(\text{TMS})_2$ 

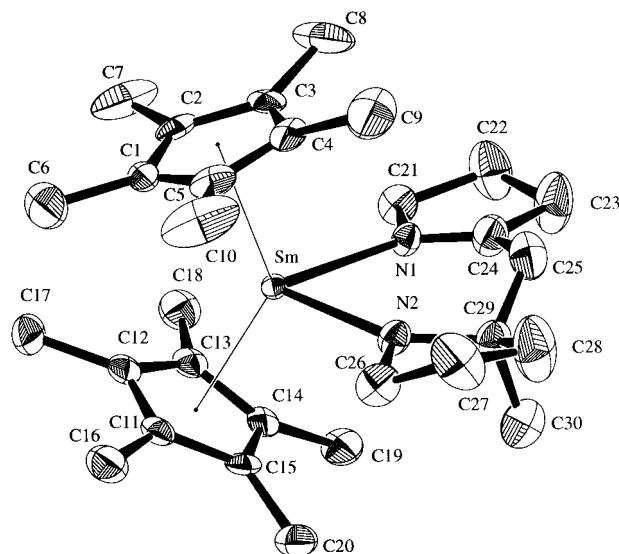
olefin transformations (including hydrogenation),<sup>8a,b,e,9f,g,10a,12a</sup> the present reductions are rather insensitive to the identity of the lanthanide (entry 1 vs entries 7 and 3 vs entries 6 and 4 vs entry 5). Furthermore, in the case of entries 1 and 8, the more “open” Sm coordination geometry actually depresses the hydrogenation rate. The observation in several NMR scale catalytic reactions of spectral features attributable to new organolanthanide complexes promoted studies of stoichiometric reactions.

**Stoichiometric Imine–Organolanthanide Chemistry.** *N*-Benzyldene(methyl)amine (**2a**). The reaction of  $\text{Cp}'_2\text{SmCH}(\text{TMS})_2$  with **2a** in toluene-*d*<sub>8</sub> (1:3.6 equiv/equiv) was monitored in the absence of  $\text{H}_2$  at 25 °C by <sup>1</sup>H NMR over the course of 136 h. The formation of two new (paramagnetic) organosamarium complexes (**4a**, **4b**) and the concurrent production of  $\text{CH}_2(\text{TMS})_2$  (useful as an internal NMR quantitation standard) are observed. Complex **4a** is formed initially, with the **4b**:**4a** ratio increasing over time and suggesting that **4b** arises from **4a**. Complex **4a** exhibits a relatively simple <sup>1</sup>H NMR spectrum with 30 Cp' (singlet), 3 Me (singlet), and 4 aryl protons (1:1:1:1) readily identifiable. The spectrum of **4b** is more complex with 30 Cp' (singlet) and 9 aryl protons detectable (see the Experimental Section for data).

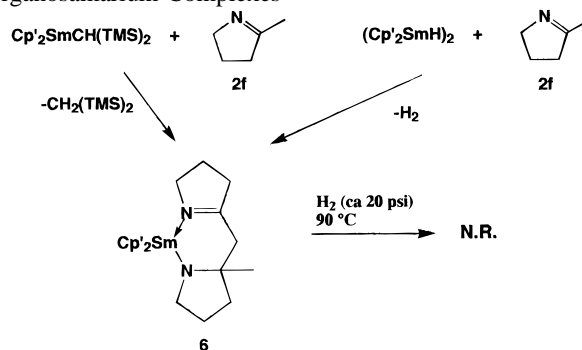
An ortho-metallated structure for **4a** (for which there is considerable precedent<sup>16,36</sup>) and an imine insertion related structure for **4b** are proposed (Scheme 2) on the basis of the NMR data and  $\text{D}_2\text{O}$  quenching/GC–MS analysis of the organic products **5a** and **5b**. Pressurizing the **4a**/**4b** reaction mixture (**4a**:**4b** ≈ 1:3) to 20 psi of  $\text{H}_2$  results in no change in the mixture composition after 22 h at room temperature. However, subsequent increase of the temperature to 90 °C effects slow diminution of the **4a** and **2a** signals (substrate hydrogenation) and negligible change in the **4b** signal. These results suggest the scenario shown in Scheme 2 in which metallated complex **4a** undergoes slow Sm–C(aryl) hydrogenolysis, while complex **4b** is more inert. Further confirmation of this scenario is provided by the observation that **2a** reacts rapidly with  $(\text{Cp}'_2\text{SmH})_2$  at 25 °C in the absence of  $\text{H}_2$  to yield a ~8:1 mixture of **4a**:**4b**. Attempts to crystallize and/or to separate **4a** and **4b** by fractional crystallization were unsuccessful.

(35) <sup>1</sup>H NMR ( $\text{CDCl}_3$ ):  $\delta$  4.82 (s, 2H,  $\text{CH}_2\text{-N}$ ), 5.40 (s, 2H,  $\text{SiH}_2$ ), 6.83–7.60 (m, 15H, phenyl-*H*). HRMS: *m/e* calcd for  $\text{C}_{19}\text{H}_{19}\text{NSi}(\text{M}^+)$  289.1287, found 289.1298.

(36) (a) Duchateau, R.; van Wee, C. T.; Teuben, J. H. *Organometallics* **1996**, *15*, 2291–2302. (b) Deelman, B.-J.; Booi, M.; Meetsma, A.; Teuben, J. H.; Kooijman, H.; Spek, A.L. *Organometallics* **1995**, *14*, 2306–2317. (c) Deelman, B.-J.; Stevels, W. M.; Teuben, J. H.; Lakin, M. T.; Spek, A. L. *Organometallics* **1994**, *13*, 3381–3391 and references therein.



**Figure 2.** Perspective ORTEP drawing of the molecular structure of complex **6**. All non-hydrogen atoms are represented by thermal ellipsoids drawn to encompass 50% probability, and hydrogen atoms are deleted for ease of viewing.

**Scheme 3.** Reaction of 2-Methylpyrroline (**2f**) with Organosamarium Complexes

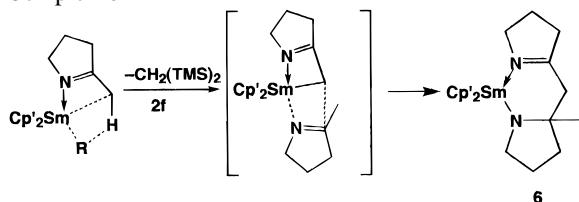
**Reaction of 2-Methyl-1-pyrroline (**2f**) with Organosamarium Complexes.** The cyclic imine 2-methyl-1-pyrroline undergoes minimal hydrogenation in the presence of  $\text{Cp}'_2\text{SmCH}(\text{TMS})_2$  (Table 1), but rather stoichiometric experiments reveal the formation of complex **6** and the evolution of  $\text{CH}_2(\text{TMS})_2$  (Scheme 3). Complex **6** can also be prepared from **2f** and  $(\text{Cp}'_2\text{SmH})_2$ , and was characterized by standard analytical techniques (the <sup>1</sup>H NMR reveals magnetically nonequivalent Cp' ligands; see the Experimental Section for details) and X-ray diffraction. Selected bond distances and bond angles are compiled in Table 3. It can be seen (Figure 2) that the molecular structure of **6** conforms closely to the  $\text{SmN}_2$  imine–amido motif shown in Scheme 3, with Sm–N<sub>2</sub>(amido) and Sm–N<sub>1</sub>(imine) distances of 2.242(4) and 2.523(4) Å, respectively. These amido–imine assignments agree with the corresponding formal C–N and C=N distances of 1.454(6) and 1.276(7) Å, respectively. The Cp' Cg–Sm–Cp' Cg angle of 132.0° and the average Sm–C(Cp') distance of 2.775(4) Å are unexceptional for  $\text{Cp}'_2\text{SmX}_2$  compounds.<sup>9f,g,37</sup>

A reasonable scenario for the formation of complex **6** invokes C–H activation at the allylic methyl position in **2f**, followed by C=N insertion into the resulting, metallacyclic Sm–C bond (Scheme 4). The former process has precedent in  $\text{Cp}'_2\text{SmR}$ -mediated activation of allylic C–H bonds in propylene and other

(37) (a) Schumann, H.; Meese-Marktscheffel, J. A.; Esser, L. *Chem. Rev.* **1995**, *95*, 865–986. (b) Evans, W. J.; Foster, S. E. *J. Organomet. Chem.* **1992**, *433*, 79–94.

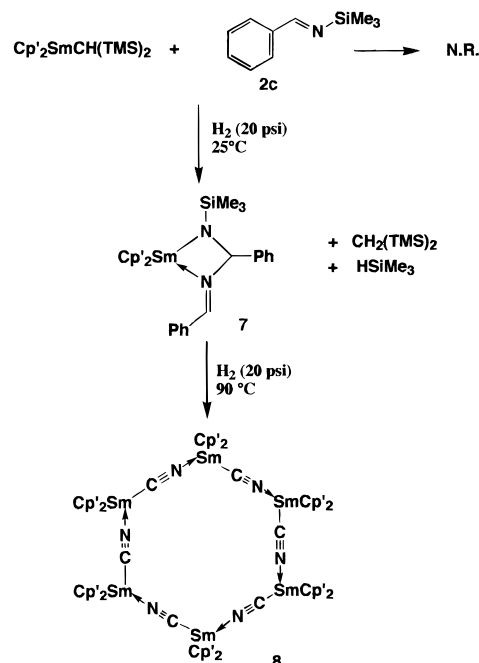
**Table 3.** Selected Bond Distances (Å) and Angles (deg) for Complex 6

Bond Distances					
Sm-N1	2.523(4)	N2-C29	1.454(6)	C12-C17	1.500(7)
Sm-N2	2.242(4)	C1-C2	1.398(7)	C13-C14	1.417(7)
Sm-C1	2.773(4)	C1-C5	1.396(7)	C13-C18	1.504(7)
Sm-C2	2.770(5)	C1-C6	1.512(8)	C14-C15	1.409(6)
Sm-C3	2.761(5)	C2-C3	1.415(7)	C14-C19	1.508(7)
Sm-C4	2.778(4)	C2-C7	1.492(8)	C15-C20	1.498(7)
Sm-C5	2.763(4)	C3-C4	1.407(7)	C21-C22	1.502(8)
Sm-C11	2.745(5)	C3-C8	1.495(7)	C22-C23	1.486(8)
Sm-C12	2.800(5)	C4-C5	1.389(7)	C23-C24	1.502(7)
Sm-C13	2.812(4)	C4-C9	1.497(8)	C24-C25	1.538(8)
Sm-C14	2.789(4)	C5-C10	1.512(8)	C25-C29	1.501(8)
Sm-C15	2.757(4)	C11-C12	1.419(7)	C26-C27	1.503(8)
N1-C21	1.478(6)	C11-C15	1.409(7)	C27-C28	1.473(9)
N1-C24	1.276(7)	C11-C16	1.506(7)	C28-C29	1.547(8)
N2-C26	1.458(6)	C12-C13	1.408(6)	C29-C30	1.533(8)
Bond Angles					
N1-Sm-N2	78.0(1)	Sm-N2-C29	135.4(3)	C26-C27-C28	103.9(5)
N1-Sm-Cg1	105.7	C26-N2-C29	106.0(4)	C27-C28-C29	107.3(5)
N1-Sm-Cg2	104.8	N1-C21-C22	107.2(4)	N2-C29-C25	112.5(4)
N2-Sm-Cg1	109.6	C21-C22-C23	105.0(4)	N2-C29-C28	104.9(4)
N2-Sm-Cg2	112.3	C22-C23-C24	103.2(5)	N2-C29-C30	111.5(5)
Cg1-Sm-Cg2	132.0	N1-C24-C23	114.6(5)	C25-C29-C28	110.5(5)
Sm-N1-C21	125.1(3)	N1-C24-C25	125.6(5)	C25-C29-C30	110.2(5)
Sm-N1-C24	126.4(3)	C23-C24-C25	119.6(5)	C28-C29-C30	107.0(5)
C21-N1-C24	108.4(4)	C24-C25-C29	116.6(5)		
Sm-N2-C26	118.5(3)	N2-C26-C27	106.0(5)		

**Scheme 4.** Plausible Reaction Mechanism for the Formation of Complex 6

olefins,<sup>9f,g,38</sup> and is likely assisted by substrate precoordination via the basic pyrroline functionality. The subsequent C=N insertion was previously observed in Scheme 2.

**Reaction of *N*-Benzylidene(trimethylsilyl)amine (2c) with Organosamarium Complexes.** In C<sub>6</sub>D<sub>6</sub> at room temperature, Cp'<sub>2</sub>SmCH(TMS)<sub>2</sub> fails to react with substrate 2c (1:8) over the course of one day. However, when the atmosphere is replaced with 20 psi of H<sub>2</sub>, the starting materials are consumed within one day at 25 °C, and complex 7 is formed in quantitative yield (Scheme 5). Concurrent formation of 1 equiv each of CH<sub>2</sub>(TMS)<sub>2</sub> and trimethylsilane is also detected by <sup>1</sup>H NMR. Complex 7 was characterized by standard analytical methods; especially noteworthy are an SiMe<sub>3</sub> signal and magnetically nonequivalent Cp' resonances in the <sup>1</sup>H NMR (see the Experimental Section for full data). The crystal structure of 7 (Figure 3) is in accord with these data and the configuration of the first product shown in Scheme 5. Selected bond distances and angles are compiled in Table 4. A Cp'<sub>2</sub>Sm fragment of unexceptional dimensions<sup>9f,g,37</sup> (average Sm-C(Cp') = 2.764(9) Å, ∠Cg-Sm-Cg = 133.0°) is incorporated in a three-membered imine-silylamido chelate ring, with Sm-N1(amido) and Sm-N2(imine) distances of 2.301(7) and 2.548(7) Å, respectively. The Sm, N1, C24, and N2 atoms are coplanar to within 0.07 Å, with a short, formal N2=C31 bond length of 1.27(1) Å and an unexceptional N1-Si1 distance of 1.711(7) Å. A possible pathway for the formation of complex 7 is depicted in Scheme 5, where desilylation proceeds via σ-bond metathesis (having precedent in lanthanide hydrocarbyl-silane chem-

**Scheme 5.** Reaction of *N*-Benzylidene(trimethylsilyl)amine (2c) with Cp'<sub>2</sub>SmCH(TMS)<sub>2</sub>

istry<sup>9c,10a,39</sup> and in examples of lanthanide hydride cleavage of Si-O bonds<sup>40</sup> to yield a benzylidene-amido complex which undergoes subsequent C-N insertion.

The reaction of imine-amido complex 7 with 20 psi of H<sub>2</sub> at 90 °C or the stoichiometric reaction of Cp'<sub>2</sub>SmCH(TMS)<sub>2</sub> with 2c under 20 psi of H<sub>2</sub> at 90 °C yields orange crystals having only two Cp' resonances in the <sup>1</sup>H NMR (1:1) and what appear to be C≡N stretching modes at 2360 and 2332 cm<sup>-1</sup> in the IR. The crystal structure of complex 8 (Figure 4) reveals a

(39) Tilley, T. D. In *The Chemistry of Organic Silicon Compounds*; Patai, S., Rappoport, Z., Eds.; John Wiley: Chichester, 1989; Chapter 24 and references therein.

(40) Evans, W. J.; Ullbarri, T. A.; Ziller, J. W. *Organometallics* 1991, 10, 134-142.

(38) Evans, W. J.; Ullbarri, T. A.; Ziller, J. W. *J. Am. Chem. Soc.* 1990, 112, 2314-2324.

**Table 4.** Selected Bond Distances (Å) and Angles (deg) for Complex 7

Bond Distances					
Sm–N1	2.301(7)	N2–C31	1.27(1)	C14–C15	1.39(1)
Sm–N2	2.548(7)	C1–C2	1.42(1)	C14–C19	1.52(1)
Sm–C1	2.80(1)	C1–C5	1.43(1)	C15–C20	1.51(1)
Sm–C2	2.757(9)	C1–C6	1.49(1)	C24–C25	1.53(1)
Sm–C3	2.744(8)	C2–C3	1.41(1)	C25–C26	1.39(1)
Sm–C4	2.765(8)	C2–C7	1.50(1)	C25–C30	1.38(1)
Sm–C5	2.803(9)	C3–C4	1.43(1)	C26–C27	1.37(1)
Sm–C11	2.753(9)	C3–C8	1.50(1)	C27–C28	1.38(1)
Sm–C12	2.759(9)	C4–C5	1.41(1)	C28–C29	1.38(1)
Sm–C13	2.761(9)	C4–C9	1.50(1)	C29–C30	1.39(1)
Sm–C14	2.754(8)	C5–C10	1.52(1)	C31–C32	1.46(1)
Sm–C15	2.743(8)	C11–C12	1.42(1)	C32–C33	1.37(1)
Si–N1	1.711(7)	C11–C15	1.42(1)	C32–C37	1.38(1)
Si–C21	1.88(1)	C11–C16	1.52(1)	C33–C34	1.38(1)
Si–C22	1.862(9)	C12–C13	1.41(1)	C34–C35	1.36(1)
Si–C23	1.87(1)	C12–C17	1.49(1)	C35–C36	1.39(1)
N1–C24	1.44(1)	C13–C14	1.41(1)	C36–C37	1.39(1)
N2–C24	1.53(1)	C13–C18	1.49(1)		
Bond Angles					
N1–Sm–N2	58.2(2)	Sm–N1–Si	134.9(4)	N1–C24–N2	105.7(7)
N1–Sm–Cg1	112.4	Sm–N1–C24	103.3(5)	N1–C24–C25	115.6(7)
N1–Sm–Cg2	111.8	Si–N1–C24	120.1(6)	N2–C24–C25	110.4(6)
N2–Sm–Cg1	112.5	Sm–N2–C24	90.5(5)	N2–C31–C32	125.1(8)
N1–Sm–Cg2	103.6	Sm–N2–C31	152.5(6)		
Cg1–Sm–Cg2	133.0	C24–N2–C31	116.7(7)		

**Table 5.** Selected Bond Distances (Å) and Angles (deg) for Complex 8

Bond Distances					
Sm–NC1	2.517(8)	NC1–NC2	1.17(1)	C11–C15	1.41(1)
Sm–NC2* <sup>a</sup>	2.532(8)	C1–C2	1.41(1)	C11–C16	1.51(1)
Sm–C1	2.695(8)	C1–C5	1.41(1)	C12–C13	1.43(1)
Sm–C2	2.720(8)	C1–C6	1.52(1)	C12–C17	1.49(1)
Sm–C3	2.682(8)	C2–C3	1.42(1)	C13–C14	1.40(1)
Sm–C4	2.688(8)	C2–C7	1.51(1)	C13–C18	1.50(1)
Sm–C5	2.694(9)	C3–C4	1.40(1)	C14–C15	1.40(1)
Sm–C11	2.715(8)	C3–C8	1.51(1)	C14–C19	1.54(1)
Sm–C12	2.708(8)	C4–C5	1.42(1)	C15–C20	1.49(1)
Sm–C13	2.719(7)	C4–C9	1.51(1)	C21–C21* <sup>a</sup>	1.40(1)
Sm–C14	2.721(8)	C5–C10	1.50(1)		
Sm–C15	2.724(8)	C11–C12	1.40(1)		
Bond Angles					
NC1–Sm–NC2* <sup>a</sup>	108.2(2)	NC2* <sup>a</sup> –Sm–Cg1 <sup>a</sup>	100.2	Sm–CN1–CN2	170.9(7)
NC1–Sm–Cg1 <sup>a</sup>	100.0	NC2* <sup>a</sup> –Sm–Cg2 <sup>a</sup>	104.0	CN1–CN2–Sm* <sup>a</sup>	175.0(6)
NC1–Sm–Cg2 <sup>a</sup>	103.0	Cg1 <sup>a</sup> –Sm–Cg2 <sup>a</sup>	138.9		

<sup>a</sup> NC2\* and Sm\* are neighboring atoms. Cg1 and Cg2 are ring centroids.

remarkable 18-membered ring of constitution (Cp'₂Smμ-CN)₆. Selected bond angles and distances are compiled in Table 5. The Sm–C≡N and –C≡N–Sm vectors are nearly linear (see the Experimental Section for a discussion of how the C≡N disorder was treated) with angles of 170.9° and 175.0°, and the Cg–Sm–Cg angle is 138.9°—typical of Cp'₂SmX₂ complexes.<sup>9f,g,37</sup> The Sm–Sm–Sm angle in **8** is 104.8°, ∠C(N)–Sm–N(C) = 108.2°, and the conformation of the 18-membered ring is chairlike (S₆ symmetry, **8**) with fold angles of 65.19° between planes. The magnetic nonequivalence of the Cp' signals in the solution <sup>1</sup>H NMR at 25 °C suggests that the ring has low conformation mobility, presumably due to the difficulty of the bulky Cp' rings in moving past one another. The average Sm–CN–Sm distance in **8** of 6.187 Å is slightly shorter than that in the more coordinatively saturated [Cp'₂Sm(CNC₆H₁₁)(μ-CN)]₃, 6.29 Å (**9**).<sup>41</sup> Here the nine-membered [Sm(μ-CN)]₃ unit is planar to within 0.04 Å.

Scheme 7 presents one possible pathway for the conversion of complex **7** to complex **8**. Mechanistically, the least obvious step is that which creates a cyano functionality, which would

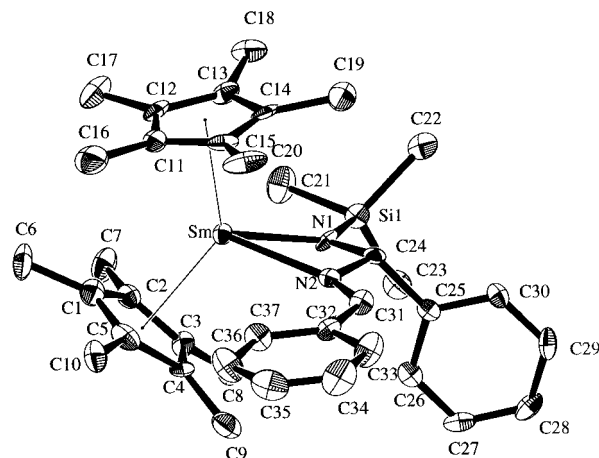


**Figure 3.** Perspective ORTEP drawing of the molecular structure of complex **7**. All non-hydrogen atoms are represented by thermal ellipsoids drawn to encompass 50% probability, and hydrogen atoms are deleted for ease of viewing.

appear invariably to require a C(β)–Ph bond scission. Scheme 7 suggests a TMSN=CPh extrusion process from the presum-

(41) Evans, W. J.; Drummond, D. K. *Organometallics* **1988**, *7*, 797–802.

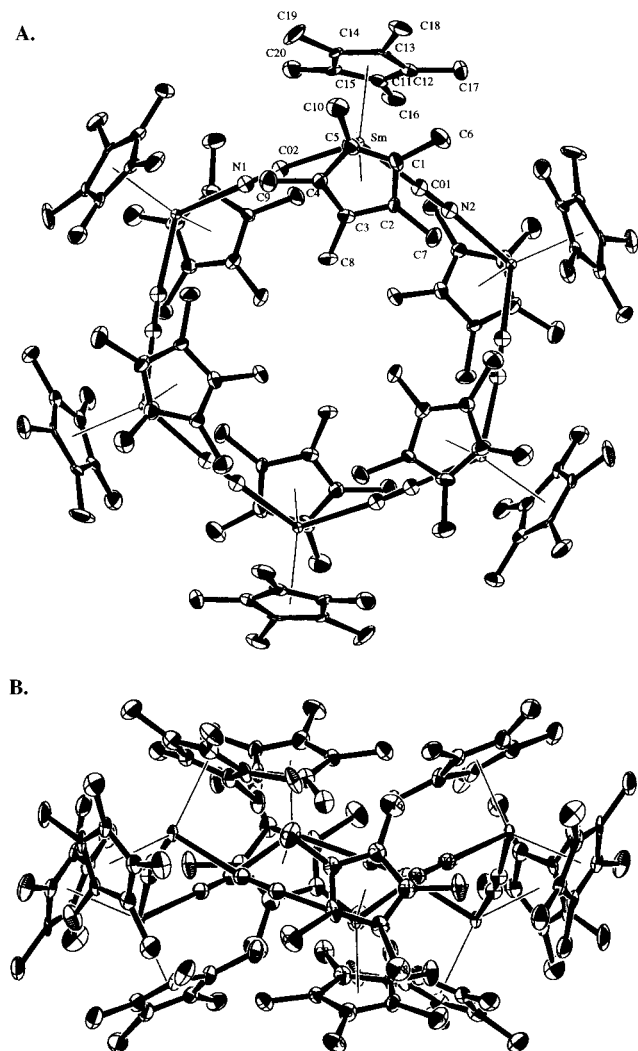
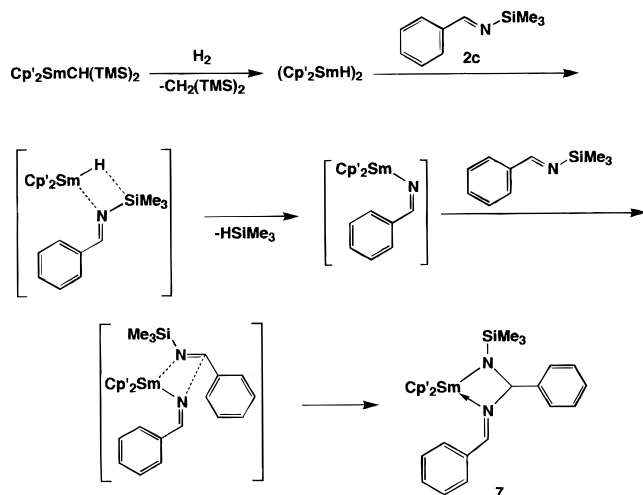


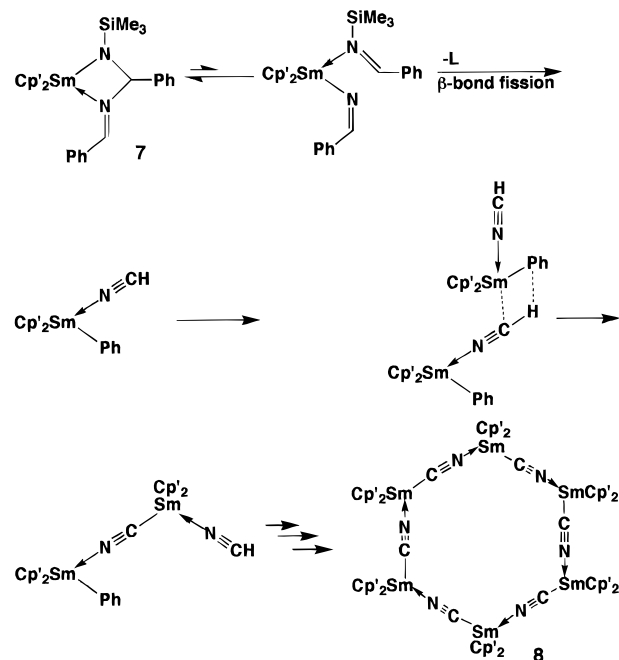
**Figure 4.** Perspective ORTEP drawing of the molecular structure of complex **8**: (A) top view, (B) side view. All non-hydrogen atoms are represented by thermal ellipsoids drawn to encompass 50% probability, and hydrogen atoms are deleted for ease of viewing. (A) is viewed along the  $S_6$  axis, and (B) is viewed perpendicular to the  $S_6$  axis.

**Scheme 6.** Plausible Pathway for the Formation of Complex **7**

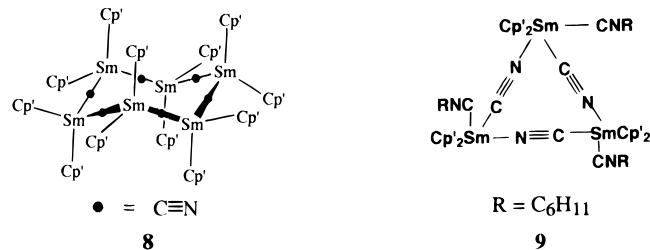


ably strained metallacycle of complex **7** (the microscopic reverse insertion process was portrayed in Schemes 2 and 4), followed by a  $\beta$ -Ph transfer to Sm. Alkyl transfer processes of this type

**Scheme 7.** Possible Pathway for the Formation of Complex **8** from Complex **7**

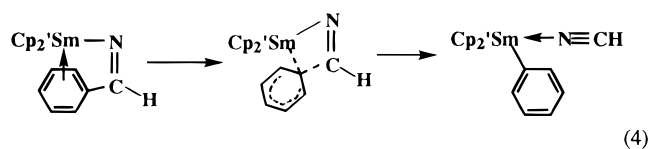


involving organolanthanide hydrocarbyls have considerable precedent.<sup>9h,13</sup> In the present case, it is possible that phenyl

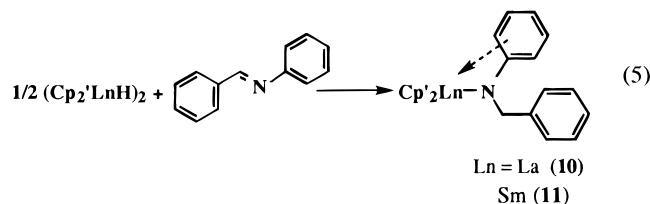


transfer is assisted through coordination of the imine and/or aryl  $\pi$ -electron system by the electrophilic lanthanide center (e.g., eq 4). Following  $\beta$ -Ph transfer,  $Cp'_2SmCN$  formation could occur via either intramolecular or intermolecular protonolytic  $C_6H_6$  elimination, followed by oligomerization (Scheme 7).

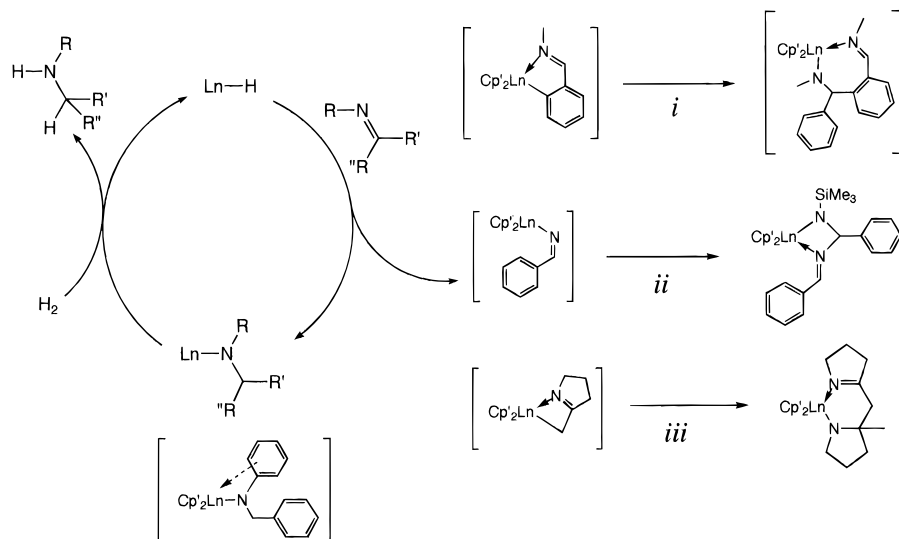
**Reaction of *N*-Benzylideneaniline (**2b**) with Organolanthanides.** Although the  $Cp'_2LnCH(TMS)_2$  complexes where  $Ln = La$  and  $Sm$  do not undergo reaction with **2b** under inert atmosphere, reaction under  $H_2$  yields insertion products **10** and



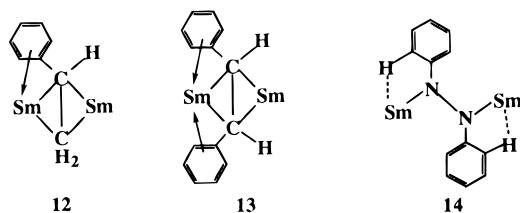
**11** (eq 5), which were characterized by standard spectroscopic



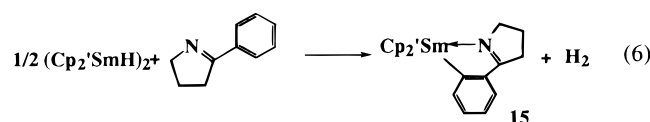
and analytical techniques (see the Experimental Section for details). The  $^1H$  NMR spectra of these complexes are straightforward; however, they exhibit slight (**10**) to very large

**Scheme 8.** Pathways for Organolanthanide-Catalyzed Imine Hydrogenation

(paramagnetic **11**) displacements of one ortho phenyl proton resonance which are suggestive of Ln interactions with either the aryl  $\pi$ -system or an ortho C–H bond. Such structures have ample precedent in organosamarium complexes of styrene (**12**),<sup>42</sup> stilbene (**13**),<sup>42</sup> and azobenzene (**14**).<sup>43</sup> Indeed, such



interactions may precede C–H activation processes such as that leading to metalation of 2-phenyl-1-pyrroline (**15**; eq 6).<sup>16</sup>

**Discussion**

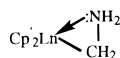
The present results demonstrate that organolanthanides are competent for the catalytic hydrogenation of acyclic organolanthanides.<sup>44</sup> Rates are modest and roughly comparable to those mediated by a chiral titanocene.<sup>7</sup> However, the organo-

(42) Evans, W. J.; Ulibarri, T. A.; Ziller, J. W. *J. Am. Chem. Soc.* **1990**, *112*, 219–223.

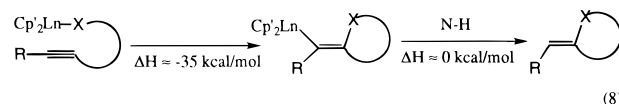
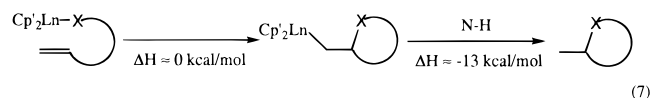
(43) (a) Evans, W. J.; Drummond, D. K.; Bott, S. G.; Atwood, J. L. *Organometallics* **1986**, *5*, 2389–2391. (b) Evans, W. J.; Drummond, D. K.; Chamberlain, L. R.; Doedens, R. J.; Bott, S. G.; Zhang, H.; Atwood, J. L. *J. Am. Chem. Soc.* **1988**, *110*, 4983–4994.

(44) Some stages of organoscandium-mediated nitrile hydrogenation appears to be similar: Bercaw, J. E.; Davies, D. L.; Wolczanski, P. T. *Organometallics* **1986**, *5*, 443–450.

(45) In principle, the initial insertion step could also proceed by the opposite regiochemistry to yield  $\text{LnCH}_2\text{NH}_2$ -type products. This reaction is actually estimated to be slightly more exothermic ( $\sim 3$  kcal/mol) than that in the schemes due to the greater product N–H bond enthalpy vs C–H. In principle, such a structure might be further stabilized by amine coordination<sup>36</sup> as shown below. Nevertheless, the NMR spectra of complexes **10** and **11** and the structures of complexes **6** and **7** are inconsistent with this regiochemistry, and an Ln–C-bonded product might be expected to give rise, in the presence of  $\text{PhSiH}_3$ , to conventional C–Si-bonded hydrosilylation products.<sup>9c,10a</sup>



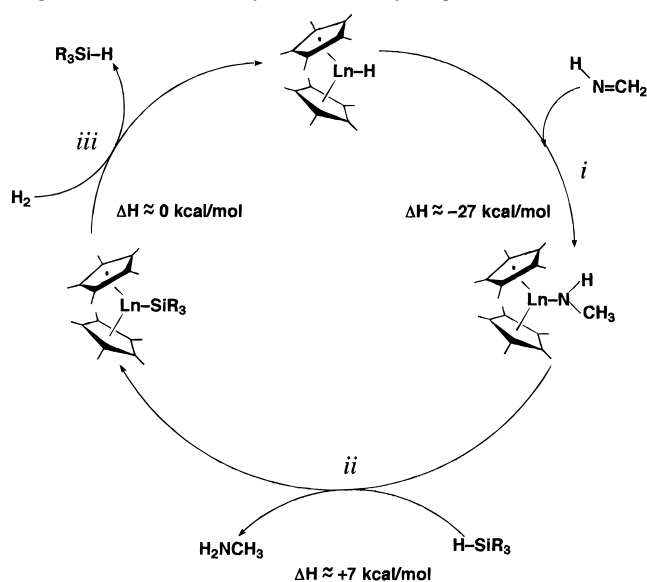
lanthanide catalysts exhibit low to negligible activity for hydrogenation of cyclic imines. In regard to mechanism, the plausible scenarios of Schemes 1, and 8,<sup>44,45</sup> a variant of pathways previously identified for organolanthanide-mediated olefin hydrogenation,<sup>8a,b,e</sup> appear reasonable. The present relative insensitivity of rates to lanthanide identity is consistent with the catalytic cycle being restricted to a single lanthanide oxidation state; however, the exact ordering has not been seen in lanthanide–olefin chemistry before.<sup>46</sup> Thus, the trends contrast with olefin hydrogenation phenomenology where, for sterically encumbered substrates, rates generally increase almost monotonically with increasing lanthanide ionic radius or more open ( $\text{Me}_2\text{SiCp}''_2\text{Ln}$ ,  $\text{Me}_2\text{SiCp}''(\text{C}_5\text{H}_3\text{R}^*)\text{Ln}$ ) coordination spheres (olefin insertion is turnover-limiting), and for  $\alpha$ -olefins, where rates increase almost monotonically with decreasing lanthanide ionic radius (metal hydrocarbyl hydrogenolysis is turnover-limiting).<sup>8e</sup> In the present case, it seems likely (as for  $\text{Ti}^{16}$ ) that the insertion step is rapid and irreversible (supported by the approximate zero-order dependence of the **2a** hydrogenation rate on  $[\mathbf{2a}]$ ), while hydrogenolysis is turnover-limiting. The exothermicity of the insertion step is consistent with a more reactant-like transition state, which might be less sensitive to steric constraints. Interesting and apparently analogous trends in lanthanide ion sensitivity are noted for organolanthanide-mediated aminoalkene and aminoalkyne cyclative hydroamination (eqs 7 and 8, X = NH, NR).<sup>14</sup> Thus, turnover-limiting,



approximately thermoneutral olefin insertion (eq 7) is appreciably accelerated by larger or more open lanthanide ions, while turnover-limiting, exothermic alkyne insertion (eq 8) is decelerated.

The present results include one example (Table 2, entry 2) where small amounts of  $\text{PhSiH}_3$  accelerate the imine hydrogenation process (in another example, competing hydrosilylation is observed; see below). It seems unlikely here that the role of

(46) For a discussion of  $\text{Ln}^{3+}$  redox characteristics, see: Morss, L. R. *Chem. Rev.* **1976**, *76*, 827–842.

**Scheme 9.** Possible Role of Silanes as Promoters in Organolanthanide-Catalyzed Imine Hydrogenation

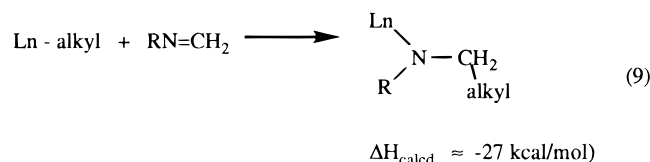
silane can be to stabilize the catalyst oxidation state. One possible role of silane may be deamidation of the lanthanide center (Scheme 9<sup>47</sup>). Protonolytic step ii has precedent in lanthanide<sup>10</sup> and group 4 hydrocarbyl<sup>38</sup> as well as possibly in group 4 amide-silane chemistry.<sup>48</sup> Hydrogenolytic step iii has precedent in organolanthanide silyl chemistry.<sup>38,49</sup> Interestingly and in analogy to the hydrocarbyl chemistry,<sup>10a</sup> transposition in the opposite sense in step ii (N → Si, H → Ln) would effect hydrosilylation of the imine.<sup>47</sup>

(47) Bond enthalpies from refs 4–6 and the following: King, W. A.; Marks, T. J. *Inorg. Chim. Acta* **1995**, *229*, 343–354.

(48) (a) Liu, H. Q.; Harrod, J. F. *Organometallics* **1992**, *11*, 822–827. (b) He, J.; Liu, H. Q.; Harrod, J. F.; Hynes, R. *Organometallics* **1994**, *13*, 336–343.

(49) Radu, N.; Tilley, T. D. *J. Am. Chem. Soc.* **1995**, *117*, 5863–5864 and references therein.

Catalytic organolanthanide chemistry almost invariably involves sequences of insertions of unsaturated species into metal–ligand  $\sigma$ -bonds coupled to/in competition with, four-center  $\sigma$ -bond metathesis processes, which transpose  $\sigma$ -bonded groups within the lanthanide coordination sphere.<sup>8–14</sup> The present study provides examples of this interplay, with exothermic, catalyst-deactivating<sup>4–6</sup> C=N insertion (eq 9) intercept-



ing products of  $\sigma$ -bond metathetical C–H activation (Scheme 8, i, iii) and C=N extrusion (Scheme 8, ii). In the case of cyclic imines, C–H activation pathways are apparently more rapid than C–N insertion (Schemes 3 and 4; eq 6), and low hydrogenolytic reactivity of the products renders imine hydrogenation at best a minor pathway. The formation of such byproducts is an obvious complication in effecting organolanthanide-catalyzed imine hydrogenations for large numbers of turnovers. Whether similar species may be of comparable importance in the group 4 catalytic chemistry is presently unclear.

**Acknowledgment.** We are grateful to the NSF for support of this research under Grants CHE9104112 and CHE9618589.

**Supporting Information Available:** Tables of positional and anisotropic thermal parameters and full tables of bond distances, angles, and dihedral angles for **6**, **7**, and **8** (111 pages). See any current masthead page for ordering and Internet access instructions.

JA963775+